

DETECTION OF TRACE METAL CONTAMINANTS IN MODEL BIOLOGICAL
TISSUE WITH LASER-INDUCED BREAKDOWN SPECTROSCOPY

by

Marian Dawn Adamson

A senior thesis submitted to the faculty of

Brigham Young University

in partial fulfillment of the requirements for the degree of

Bachelors of Science

Department of Physics and Astronomy

Brigham Young University

April 2007

Copyright © 2007 Marian Adamson

All Rights Reserved

BRIGHAM YOUNG UNIVERSITY

DEPARTMENT APPROVAL

of a senior thesis submitted by

Marian Dawn Adamson

This thesis has been reviewed by the research advisor, research coordinator, and department chair and has been found to be satisfactory.

Date

R. Steven Turley, BYU Advisor

Date

Steve Rehse, Wayne State University Advisor

Date

Eric Hintz, Research Coordinator

Date

Scott Sommerfeldt, Chair

ABSTRACT

DETECTION OF TRACE METAL CONTAMINANTS IN MODEL BIOLOGICAL TISSUE

WITH LASER-INDUCED BREAKDOWN SPECTROSCOPY

Marian Dawn Adamson

Department of Physics and Astronomy

Bachelor of Science

Researchers at Wayne State's Smart Sensors and Integrated Microsystems program are developing wireless retinal implants, but worry that these implants might be depositing aluminum into the soft surrounding tissue. Laser-Induced Breakdown Spectroscopy (LIBS) is an excellent tool for trace elemental analysis and was therefore studied as a method of detecting small amounts of aluminum in tissue. Tissue was modeled using 2% agarose gelatin and doped using nanoparticle aluminum oxide solution. LIBS was effective at detecting very low concentrations of aluminum in this model biological tissue. A calibration curve created from standardized samples with well-known Al concentrations was made and determined to be linear. A limit of detection, extrapolated from the calibration curve, was found to be less than 1 ppm. Also studied were rates of false negatives and false positives for a much more realistic testing methodology: few

accumulations on a low aluminum concentration sample. For a 2 ppm aluminum sample, 45% of the measurements gave false negatives for a single accumulation measurement, but only 20% gave false negatives for a two accumulation measurement. The low limit of detection and relative sensitivity at few accumulations show that LIBS is an excellent tool for detecting aluminum in a tissue stimulant. This method should be further investigated for use as an *in vivo* analysis tool.

ACKNOWLEDGMENTS

I would like to acknowledge Dr. Steven Rehse for his many hours of patient teaching and explaining, as well as for the use of his equipment. I also like to thank Dr. R. Steven Turley for being an excellent teacher, for supporting my decisions, and for helping me achieve this degree with some creative thinking. I would like to thank Nichole Van Valkenburgh for critiquing my thesis with a non-science eye. Finally, I would like to thank my husband for the opportunity to do this research at all.

Contents

CONTENTS	VII
LIST OF FIGURES	VIII
CHAPTER 1: INTRODUCTION	1
LASER-INDUCED BREAKDOWN SPECTROSCOPY	1
BIOLOGICAL IMPLANTS	2
PHYSICS OF LIBS	3
<i>Overview</i>	3
<i>Atomic Physics</i>	4
<i>Assumptions</i>	5
CHAPTER 2: EXPERIMENT	7
MODEL TISSUE	7
<i>Choosing the Material</i>	7
<i>Doping with Aluminum</i>	8
<i>Sample Creation Methodology</i>	9
LIBS APPARATUS	10
<i>Laser Delivery</i>	11
<i>Sample Placement</i>	12
<i>Light Collection and Analysis</i>	13
<i>Experimental Variables</i>	13
CHAPTER 3: ANALYSIS AND RESULTS	15
TYPICAL SPECTRA	15
CONCENTRATION CURVES.....	16
<i>Measurement Method</i>	16
<i>Analysis Method</i>	17
<i>Final Concentration Curves</i>	<i>Error! Bookmark not defined.</i>
LIMIT OF DETECTION.....	21
<i>Reducing the LOD</i>	22
<i>Final Limits of Detection</i>	23
FEW ACCUMULATION MEASUREMENTS	24
<i>Few Accumulations Data Analysis</i>	25
<i>Data for Few Accumulation Measurements</i>	26
CONCLUSION	28
BIBLIOGRAPHY	31
APPENDIX A. SINGLE ACCUMULATION ANALYSIS MATLAB CODE	34

List of Figures

FIGURE 1. THE STRUCTURE OF THE GROUND STATE AND FIRST EXCITED STATE OF ALUMINUM.	5
FIGURE 2. A 2% AGAROSE (NO AL) SAMPLE WITH MULTIPLE LINES OF LASER ABLATION. THE RING ON THE TOP LEFT OF THE SAMPLE IS DUE TO THE HEIGHT ALIGNMENT SCREW.	10
FIGURE 3. THE EXPERIMENTAL APPARATUS USING TWO CYLINDRICAL LENSES TO ABLATE THE MODEL TISSUE.	10
FIGURE 4. TWO CROSSED CYLINDRICAL LENSES CREATING A LINE OF ABLATION ON THE SAMPLE.	12
FIGURE 5. A SPECTRUM TAKEN FROM A 60 PPM SAMPLE DISPLAYING THE ENTIRE RANGE OF THE SPECTROMETER. ($\tau_D = 6\mu\text{s}$, $\tau_w = 20\mu\text{s}$, 80 MJ/PULSE, 3 OCA, AMP = 2800, 38 ACCUMULATIONS)	15
FIGURE 6. THE SAME SPECTRUM ZOOMED IN AROUND THE AL AND CA PEAKS.	16
FIGURE 7. CONCENTRATION CURVE OF AL/CA (80 MJ/PULSE, $\tau_D = 6\mu\text{s}$).	18
FIGURE 8. THE LOCATION OF THE CROSS BETWEEN THE FIT OF THE UPPER REGIONS AND THE FIT OF THE LOWER REGIONS.	19
FIGURE 9. GRAPH OF CA INTENSITY VERSUS AL CONCENTRATION	20
FIGURE 10. CONCENTRATION CURVE OF AL WITH NO REFERENCE LINE (80 MJ/PULSE, $\tau_D = 6\mu\text{s}$).	21
FIGURE 11. THE EFFECT OF DELAY TIME (A) AND LASER ENERGY (B) ON THE NOISE, σ , OF THE SAMPLE.	23
FIGURE 12. TABLE OF THE LIMIT OF DETECTION (LOD) AND ITS COMPONENTS FOR FIGURES __ AND __.	24
FIGURE 13. SINGLE ACCUMULATION MEASUREMENT ON A 2 PPM AL SAMPLE. THE TWO MIDDLE ARROWS DENOTE WHERE THE ALUMINUM SHOULD APPEAR. THE OUTSIDE ARROWS SHOW THE TWO CALCIUM PEAKS.	25
FIGURE 14. PERCENTAGES OF “YES” AND “NO” FOR A SINGLE ACCUMULATION SYSTEM. THE CRITERION FOR THE ALUMINUM SIGNAL WAS 3σ , AND THE LASER ENERGY IS 80 MJ/PULSE.	27
FIGURE 15. THE CHANGE IN “YES” AND “NO” PERCENTAGES WITH INCREASING ACCUMULATIONS. THE CRITERION HERE IS AL SIGNAL ABOVE 3σ , THE LASER ENERGY IS 80 MJ/PULSE, AND THE SAMPLE IS 2 PPM AL.	28

Chapter 1: Introduction

Laser-Induced Breakdown Spectroscopy

Laser-Induced Breakdown Spectroscopy, LIBS, is an optical spectroscopic technique used to determine the elemental make-up of a target. In LIBS, a high-intensity, pulsed laser is focused on the material of interest, first vaporizing the material and then breaking atoms into ions creating a small plasma. Light is created by ions and atoms falling from excited states via spontaneous emission and is collected into a spectrometer. The resulting spectrum of intensity versus wavelength shows peaks at the characteristic wavelengths of the atoms and molecules in the material. LIBS is done on all types of materials, solid, liquid, or gas. Some of its many advantages are little sample preparation, little harm to the sample, short data analysis time, and its excellence in detecting even trace amounts of metals.

LIBS is used for many applications like testing for pollution [1-3], determining alloy constituents concentration [4], and 2-D elemental mapping [5]. Especially interesting are LIBS applications for biological systems. Others have done research to identify malignant tissue [6], study teeth and bones [7], and probe microbiological systems [8]. To my knowledge, little to no research has been done using LIBS to detect elements in human tissue. However, this area has much potential. The advantage of LIBS over other tissue analysis methods is its ability to quickly and almost harmlessly test a material. Other methods require sending tissue removed by a biopsy to a lab, and results arrive days or weeks later. LIBS also has great potential for studying tissue *in*

vivo using fiber optic laser delivery and light collection. By inserting a tiny fiber-optic cable and using LIBS, tissue could be tested for composition anywhere in the human body.

Biological Implants

Amazing research is being done studying biological implants at the Smart Sensors and Integrated Microsystems program at Wayne State University. These implants have the potential to do everything from restore sight and muscle operation to automatically release pressure in the brain. They often are tiny microchip sensors that detect and send information to the doctor or the body itself. One chip, for example, would sit on the back of the retina and send electrical pulses to the brain [9]. It is important to research the effects of a sensor placed in tissue for a long period of time because the body tends to attack any foreign object placed in it. The sensor must be inert and not react with any biological tissue. For this reason, sapphire, Al_2O_3 , which has good optical qualities as well as being hard and inert, is often used. However, these sapphire substrate retinal implants tend to quit working with time. One supposition is that aluminum is being deposited from the sensor into the tissue. This could cause the mechanism to fail and also deposit harmful metals into the tissue.

I studied the use of LIBS as a test mechanism to examine whether metals are diffusing out of a biosensor into surrounding tissue. LIBS was applied to a tissue-like target seeded with metal and efforts were made to see aluminum in the sample, create an aluminum concentration curve, determine a limit of detection, and test the limit of detection. This report discusses the experimental methods and conclusions for these tests

and ultimately answers the question: Can LIBS be used to determine trace concentrations of aluminum in human tissue, and can this be developed for *in vivo* studies?

Physics of LIBS

Overview

In LIBS, a high-intensity, pulsed, infrared laser is focused on a material and forms a plasma by non-resonant processes. Early in the pulse the material is vaporized by depositing large amounts of thermal energy. At later times, the pulse photons, which are not energetic enough to ionize atoms on their own, give energy to free electrons by reverse bremsstrahlung. As these increasingly energized electrons collide with other objects in the vapor, an electron cascade occurs and quickly causes the breakdown of the vapor into a plasma with temperatures of 10,000 to 20,000 K and electron densities of $10^{17} - 10^{20} \text{ cm}^{-3}$. As the plasma cools, the many ions, atoms, and molecules fall back to their ground state configurations, losing energy as photons. Directly after laser ablation (0 to 0.5 μs) the plasma emits broadband continuum radiation from bremsstrahlung and ionized electrons being captured back into atoms. This background then dies down revealing the characteristic emissions from both atoms that are no longer ionized and remaining ions (0.5 to 4 μs). After even longer times (4 to 20 μs) atoms rejoin into molecules, and emissions from these molecules can be seen. Thus, LIBS is a time-resolved technique, and, by changing the wait time after the laser ablation and before light collection, called the delay time, one can analyze different parts of the material. Typically, a LIBS user is most interested in the atomic emissions. These emissions occur when an electron falls from an excited state down into a lower or ground state. These states have specific, quantized energies, and therefore the difference between levels is

also distinct. When the electron loses energy, conservation of energy requires that the energy goes somewhere, and so a photon is emitted with the exact same amount of energy as the difference between energy levels. These photons are spectrally dispersed by a spectrometer and detected by an ICCD camera.

The data is displayed as a spectrum of intensity versus wavelength. Various photons from the same energy transition within an atom have more or less the same energies and so form an intensity peak in the wavelength spectrum. This peak is very narrow and is often called an atomic emission “line.” Realistically, the peaks are only so narrow and are broadened by various effects: Doppler shifting of light coming from very hot, fast-moving atoms, saturation, instrument response, etc. The spectrum is analyzed by studying these emission lines to determine what elements are in the material. Information on the characteristic emissions from atoms can be found easily using, for example, the NIST or Kurucz tables online [10,11]. Unluckily, noise “lines” also occur for whatever reason and these must be discriminated against. Atomic emissions can overlap with other atomic emissions and molecular emissions which appear as broad comb-like structures. Therefore understanding an emission spectrum can be tricky business.

Atomic Physics

In the plasma created by the laser, thermal energy has ripped molecules apart and electrons off of the atoms. As the plasma cools, the bits and pieces start to recombine releasing energy as photons. First electrons fall back to the outer shells, making the atoms no longer ionic, but still excited. Then more photons are emitted as the atoms return to their ground states. Finally, the atoms recombine into molecules and the “laser

splatter” falls back onto the surface of the material. The interesting emission lines for this study are the resonance lines of aluminum, 394.4 and 396.1 nm, meaning they are the last transition some electrons make as they fall back into the ground state. These electrons are coming from the $4s^2S_{1/2}$ state. The lowest energy level has fine structure splitting, so the electrons have a choice of which state to fall into, $3p^2P_{3/2}$ or $3p^2P_{1/2}$. (See Figure 1.) They follow the probabilities set forth by quantum mechanics having a branching ratio of 2:1. So, 66% of the time they fall to the 396 line and 33% they fall to the other. Therefore, the 396.1 line is bigger and easier to detect.

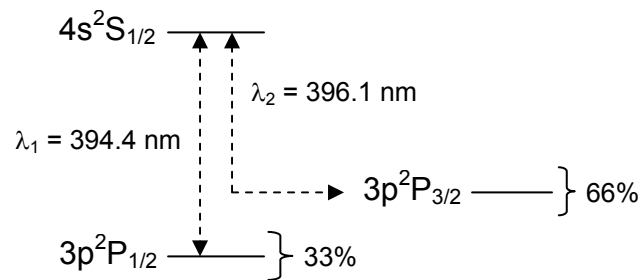


Figure 1. The structure of the ground state and first excited state of aluminum.

Assumptions

In order to acquire information from LIBS some assumptions are required. The first assumption is local thermodynamic equilibrium, LTE. This means that any area of a small region is essentially the same, and any information from that area is representative of the whole region. In order for this to be true, the electron density must be great enough to cause many collisions per second, creating a uniform temperature. A second assumption is that the spark is optically thin. This means that light from one area of the plasma plume will not be blocked from the detector by a different area. This assumption

can be tested by determining the ratio of two emission lines of the same element. The ratio of these lines is set by quantum physics and should not change if the plasma is optically thin. The ratio of the two aluminum resonance lines, as stated above, is 2:1, and a study of these two peaks shows that this ratio holds. A third, less true assumption is that the entire spark is uniform. Other researchers have probed the different parts of the laser plasma and found this not to be true [12]. However, our system collects light from the whole spark, so this assumption is necessary. The third assumption is that there is no self-absorption of the aluminum resonance lines used for this study. This is an acceptable assumption since the aluminum in the plasma is very dilute. These four assumptions are necessary for obtaining and analyzing the data, which are discussed in the following two chapters.

Chapter 2: Experiment

There were two main sections of the experiment to develop: the sample and the LIBS apparatus. The sample needed to model soft tissue, contain known amounts of aluminum, and have a standardized creation methodology. The LIBS apparatus required equipment for laser delivery, holding the sample, and light collection. These are all discussed below.

Model Tissue

While the project's goal was to study the use of LIBS on human tissue, it was preferable to use a model biological tissue for this preliminary experiment. When using real tissue complications arise in how to obtain it, store it, and dope it with known amounts of aluminum. By making a model tissue, LIBS could be easily tested for this application before addressing these and other issues. Therefore, before any LIBS research could be done, a matrix to model human soft tissue needed to be researched and made.

Choosing the Material

The human tissue of most interest in this experiment is soft tissue located around the eyes. This soft tissue is largely water and contains the elements C, H, N, and O [13]. As LIBS is an elemental analysis tool, any human tissue model tested with this technique must contain these elements. (Our samples also ended up have large amounts of Na and Ca, but these elements are also contained in the human body and do not propose a

problem. In fact, as shown later, Ca was extremely useful.) A literature search shows that previous researchers (not in LIBS fields) have used mediums such as gelatin [13-15], agarose [15,16], carrageenan [15], and agar [15] to model human tissue. All of these form gels, meaning a jello-like material, under the right conditions. The two most popular mediums were chosen because they were easy to obtain and cheap: electrophoresis grade agarose (BP161-100, Fisher Chemical) and gelatin (Knox, Terrytown, NY). Both were made into gels and tested using LIBS. The two had comparable spectra, and so agarose was chosen because it didn't mold as easily.

Doping with Aluminum

The goal of this project was to determine the ability of LIBS to detect the concentration of aluminum in tissue. Therefore, known amounts of aluminum needed to be uniformly distributed throughout the agarose samples. A first method, mixing in dry micron-sized aluminum particles (266515-5G, Sigma-Aldrich), was discarded because 1) the particles settled to the bottom during gel solidification leaving an unknown concentration in the sample, and 2) the particles were a large fraction of the spot size of the focused laser causing non-uniformities from measurement to measurement. A second method, mixing in an aluminum-oxide nanoparticle water solution (#12733, Alfa Aesar), was much more successful. The tiny aluminum-oxide particles remained indefinitely in suspension even in water. In fact, the dispersed particles caused the water solution to be milky white due to diffraction effects, and when added, the sample would also become milky as the particles remained in suspension. The tiny particles were miniscule in comparison with the laser spot size and helped increase the reproducibility from measurement to measurement. Plus, aluminum was 8.996% of the $\text{Al}_2\text{O}_3\text{-H}_2\text{O}$ solution,

making it easier to add tiny amounts of aluminum by measuring macroscopic amounts of solution.

Sample Creation Methodology

After much trial and error, a specific gel creation methodology was developed. First, 2 g of agarose powder were added to a 200 mL beaker to be 2% of the final mixture. A small amount of aluminum solution was measured into a small glass vial. Ultrapure water (<1 ppm trace contaminants, <20 M Ω , Omnipure and U.S. Filter, Purelab Plus UV/UF) was then poured into the vial, and the vial was emptied into the beaker. This was repeated several times to remove the somewhat sticky aluminum solution from the vial. The beaker was then filled with ultrapure water until the whole mixture weighed slightly more than 100 g (to allow for evaporation). A large magnetic stir rod was added, and the beaker was placed on a magnetic stirring hot plate. All weights were carefully recorded. The mixture was stirred at 150 rpm and heated at 200°C until the agarose dissolved at a temperature around 87°C. The mixture was then removed, weighed again to determine water evaporation, and poured into a Petri dish with an 8 cm diameter. The dish was swirled to decrease the meniscus and left untouched and open to air for a couple hours to cool and dry. Major evaporation of the final sample occurred if left uncovered for long amounts of time, and so the sample was kept covered after this initial drying time. The finished gel was firm and could be lifted as one piece. Because the top surface of the gel was subject to curvature, bubbles, and other irregularities, the sample was cut out of its dish and carefully turned over to expose the very flat bottom side for laser ablation. Figure 2 shows a finished 2% agarose sample with ablation on it.



Figure 2. A 2% agarose (no Al) sample with multiple lines of laser ablation. The ring on the top left of the sample is due to the height alignment screw.

LIBS Apparatus

The LIBS system can be broken into three main parts: laser delivery, sample and holder, and light collection/analysis. The system is shown schematically in Figure 3.

Each part is discussed below along with the experimental variables used.

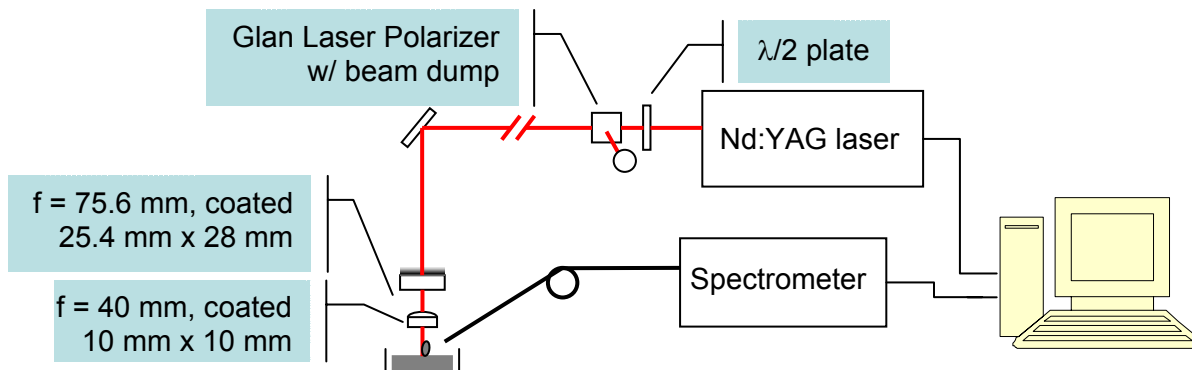


Figure 3. The experimental apparatus using two cylindrical lenses to ablate the model tissue.

Laser Delivery

Our system used an (infrared) Nd:YAG laser (Spectra-Physics) at its fundamental frequency of 1064 nm. Light was emitted as 10 ns pulses at a 10 Hz repetition frequency and had an average energy of 650 mJ/pulse. However, typical experimentation was done from 10 to 100 mJ/pulse. The energy of the light was reduced using a half-wave plate and a Glan Laser Polarizer. We could control the amount of light exiting the polarizer by turning the half-wave plate. The light was then directed to the experiment using turning mirrors coated for high-reflectance at 1064 nm.

Two methods of laser delivery were tested for reproducibility and signal strength. The first of these used a 5x microscope objective to focus onto the sample. The spot size from the objective was 100 μm in diameter. The second method used a cylindrical lens ($f = 40$ mm, coated, 10 mm by 10 mm) to focus the laser. Cylindrical lenses focus light in only one dimension and create a line on the sample. Our line had the same width as the objective spot, but was about 1 mm in length. This extra ablated area was useful because it allowed for more averaging and more created light, thus enhancing the reproducibility. A second cylindrical lens ($f = 75.6$ mm, coated, 25.4 mm by 28 mm) was placed over top of the first with its length axis crossed with the length axis of the first. This simply controlled the length of the line and assured that no power was lost on the edges of the main lens. Figure 4 shows two crossed cylindrical lenses and how they reduce the beam to a line.

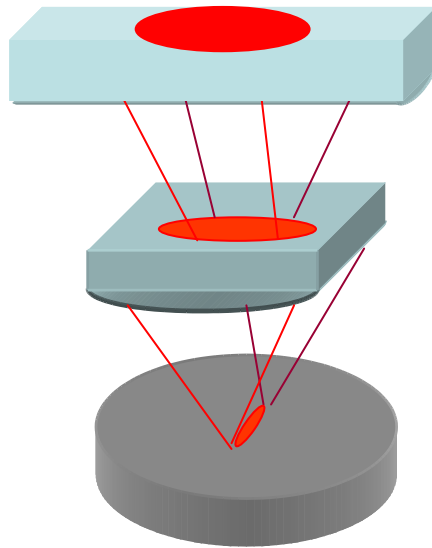


Figure 4. Two crossed cylindrical lenses creating a line of ablation on the sample.

Sample Placement

The sample was held by a platform attached to three translation stages for ease in alignment and area selection. The distance from the lens to the sample was extremely important as a variation of 0.01" could change the resulting spectrum. Sample height was set in the following way: A screw attached the lens holder was brought down to touch a previously aligned sample. This sample was then lowered and removed, and a new sample was inserted and raised until it touched the screw. The screw was then moved up out of the way. Measurements at single locations (which consisted of 3 laser shots on the same location with spectra added together on the ICCD camera) were taken while changing the height small amounts at a time. The focus of a lens is the narrowest region of the beam waist. Therefore, the smallest laser spots on the sample corresponded to the best location of the top surface with respect to the beam focus. Once a good height region was determined using the spot size, spectra were taken at even intervals within

that height region and compared. A spectrum and corresponding height were chosen by picking the largest ratio of the carbon line at 247 nm to the sodium doublet at 589 nm and also the largest absolute intensity of the calcium lines at 393 nm and 396 nm. If the sample contained aluminum, a large absolute intensity of the aluminum 396 nm and 394 nm lines was also considered good. Often, a well aligned sample showed increased intensity throughout the entire spectrum.

Light Collection and Analysis

Light was collected via an optical fiber (steel encased multimode) placed at a distance of 23 mm from the ablation spot without any lenses. Fiber alignment was typically completed by coupling a HeNe laser into the opposite end and allowing the resulting light at the sample end to cover the area of ablation. The opposite end would then be replaced on the spectrometer for measurement. The spectrometer was an ESA 2000 Eschelle spectrometer (LLA Instruments, Inc) with a wavelength range of 200 to 800 nm and a resolution as good as .005 nm in the ultraviolet range. It was equipped with a charge coupled device (CCD) camera for light collection. (See **Error! Reference source not found.** for the entire apparatus.) The excellent resolution of this relatively new type of spectrometer allowed for excellent detection of very small emission lines and is a great improvement over early LIBS experiments' resolution. The laser and spectrometer could both be controlled using a computer program called ESAWIN which came with the spectrometer.

Experimental Variables

Besides the simple geometrical parameters of the setup, there were various other important parameters to optimize. They will be defined here and used in later discussion.

Common to all LIBS applications:

- Laser energy, measured in mJ/pulse, is the energy of the laser after it has been reduced using the polarizer. More laser energy created more characteristic light, but also more background light.
- Delay time or gate delay, τ_d , is the period of time between the laser shot and light collection and, by varying, can allow study of light emission over time.
- Gate width, τ_w , is the period of time the spectrometer collects spark light, starting at the delay time after the laser pulse.

Used specifically in our system:

- On chip accumulations, OCA, is the number of laser shots taken at one sample location and allowed to accumulate on the CCD camera before the data is read into the computer.
- Accumulations, the number of spectra averaged together by the computer program ESAWIN. These were typically spectra from laser shots at different locations on the sample.
- Amplification, amp, the boost given the CCD camera to increase signal before being read onto the computer.

Chapter 3: Analysis and Results

Using the above apparatus and model tissue, LIBS was performed to obtain spectra which held information about the aluminum in the system. By analyzing these spectra, a concentration curve was made, the limit of detection determined, and the method's feasibility for small area analysis was tested.

Typical Spectra

Figure 5 displays a typical LIBS spectrum for the entire range seen by the spectrometer, 201 nm to 836 nm. The most prominent lines are labeled. The smaller region in Figure 6 from 393.00 nm to 397.25 nm contains the aluminum and calcium lines of most interest. The right-most aluminum line at 396.152 was used for analysis, and the left-most calcium line at 384.366 was sometimes used as a reference line.

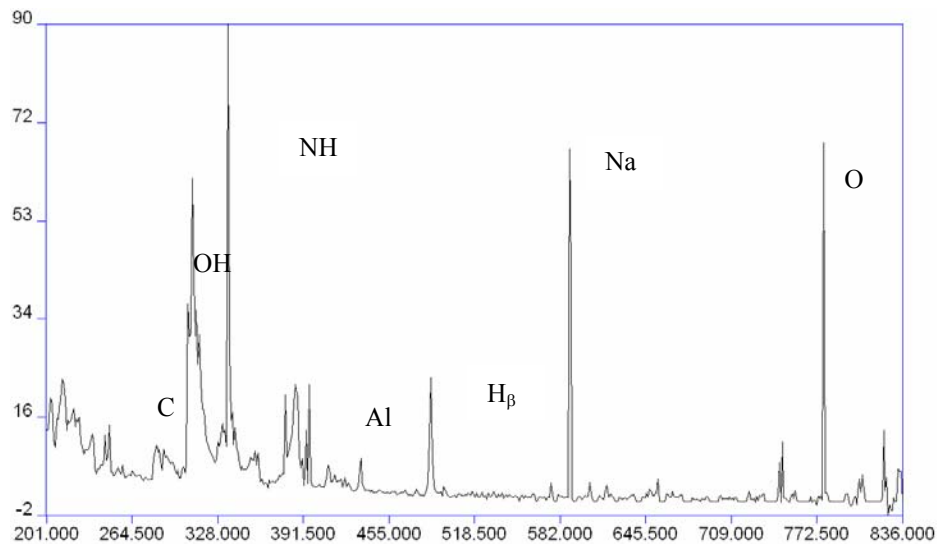


Figure 5. A spectrum taken from a 60 ppm sample displaying the entire range of the spectrometer. ($\tau_d = 6\mu\text{s}$, $\tau_w = 20\mu\text{s}$, 80 mJ/pulse, 3 OCA, amp = 2800, 38 accumulations)

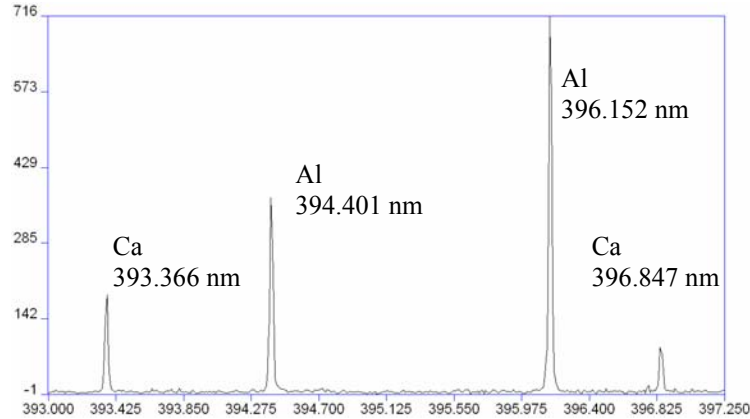


Figure 6. The same spectrum zoomed in around the Al and Ca peaks.

Concentration Curves

The first goal of the project, after simply seeing the aluminum peaks, was to create a concentration curve, a graph showing the functional relationship between the measured Al line intensity and the concentration of Al in a sample.

Measurement Method

The curve was made from standard samples each containing different known concentrations of aluminum ranging from 10 ppm to 1000 ppm. One “measurement” consisted of 40 accumulations. Each accumulation consisted of 3 laser shots in one location producing a single spectrum. (See Figure 2 above to see multiple lines of 40 laser shots.) Forty of these spectra were averaged together to create one spectrum, as seen in Figure 5. Then, for each concentration 10 to 13 measurements were taken. All data was taken with $\tau_d = 6\mu\text{s}$, $\tau_w = 20\mu\text{s}$, 80 mJ/pulse, and amp = 2800.

Analysis Method

The measurement spectra were analyzed by fitting the aluminum and calcium peaks and finding the area under the curves. Since the concentration curve was a comparison between lines of different concentrations, any method could be used to compute the intensity, as long as it was consistent and logical. The program that controlled the data collection and display, ESAWIN, also provided a concentration curve plotter. The program could take a set of multiple measurements for multiple concentrations in their original form and create a calibration curve of Al/Ca intensity to concentration. (The spectrum files had to be modified before using in any other program.) This method was compared to a more manual method using Fortran which performed a numerical integration of the peak, and the two agreed.

Final Concentration Curves

Figure 7 is a graph of intensity versus concentration for a range from 10 ppm to 1000 ppm. The intensity is a normalized intensity, aluminum at 396.152 nm divided by calcium 393.366 nm, and therefore has no units. The spread of points at each concentration corresponds to the ten measurements. The central point is the average of these ten points and is fitted to a line. The error bar on the average point is the standard deviation of the 10 individual measurements at that concentration. The error on any one measurement is 19.005%.

A weighted non-linear least squares fit was used to fit a line to the averages. We checked for saturation at high concentrations by attempting to fit the upper and lower regions with different lines. When saturation occurs a non-linear relationship between

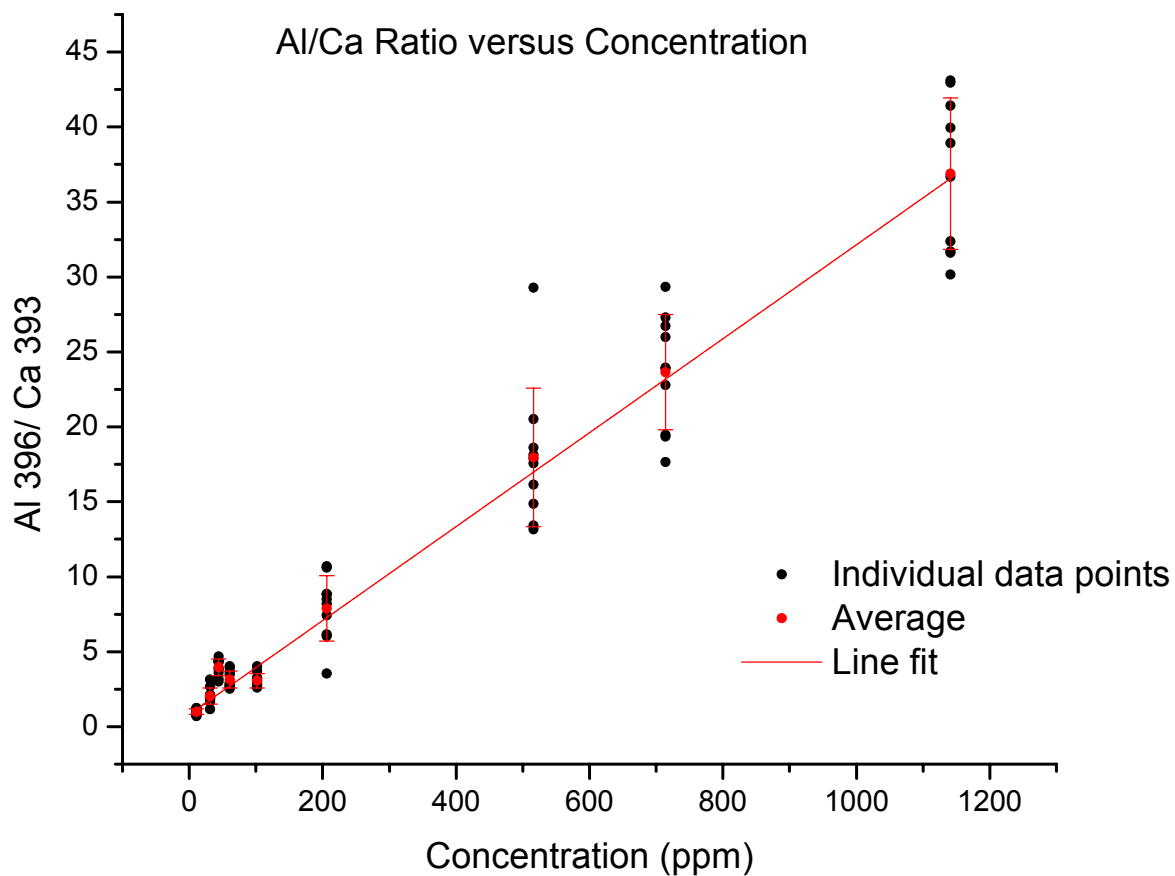


Figure 7. Concentration curve of Al/Ca (80 mJ/pulse, $\tau_a = 6 \mu s$).

intensity and concentration exists at high concentrations due to self-absorption of the lines. The following figure (Figure 8) shows an attempt to use two fits, a fit of the higher concentration region and a fit of the lower. These two lines cross at a concentration of about 40-50 ppm, corresponding to a change of linearity at this concentration. However, it is highly unlikely that saturation occurs at such a low concentration, as other studies have shown much higher saturation regions or none at all [1,17]. Therefore, it was decided that the system shows a linear relationship between 10 and 1000 ppm, and slight

changes in slope at low concentration are simply due to non-uniformities between samples. The single line fit to the whole region produced a coefficient of determination of $R^2 = 0.89536$ out of a maximum of one.

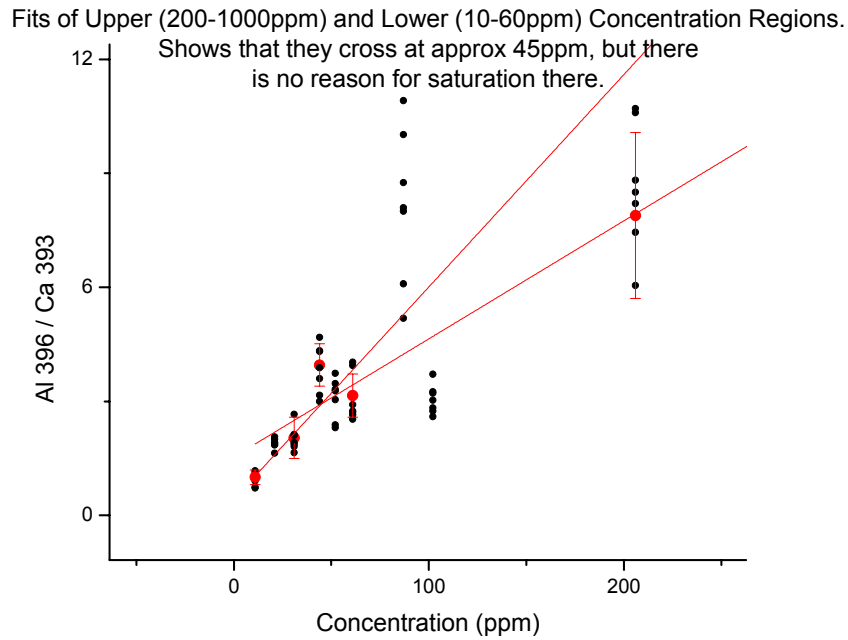


Figure 8. The location of the cross between the fit of the upper regions and the fit of the lower regions.

It is important to reference the aluminum line to another line because of non-uniformities in the sample, sample placement, and plasma intensity. A reference line should remain consistent as the aluminum concentration varies. Figure 9 shows the intensity of the reference Ca line as a function of sample's aluminum concentration. The sample with 100 ppm Al was accidentally dried out and then re-hydrated. Although this sample looked the same after re-hydration, it clearly produced a different spectrum. This mistake was fortuitous because it showed the Ca line's ability to correct for sample

inconsistencies and displayed the dependence of the spectrum on sample hydration. The noise in the lower concentration region could likely be due to small differences in sample hydration.

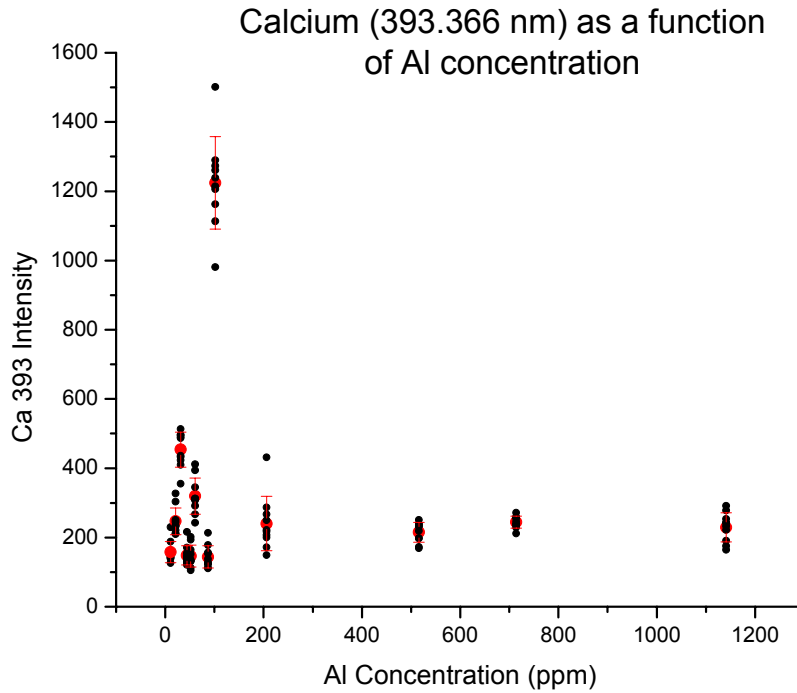


Figure 9. Graph of Ca intensity versus Al concentration

Although it can be useful to compare aluminum to a reference line, this may not always be feasible. For example, calcium concentration is doubtless different for different people. Figure 10 shows a concentration curve of aluminum intensity without the calcium reference. The curve is quite smooth, with a R^2 for the fit of 0.8978 and a fractional error on each point of 13.7695%.

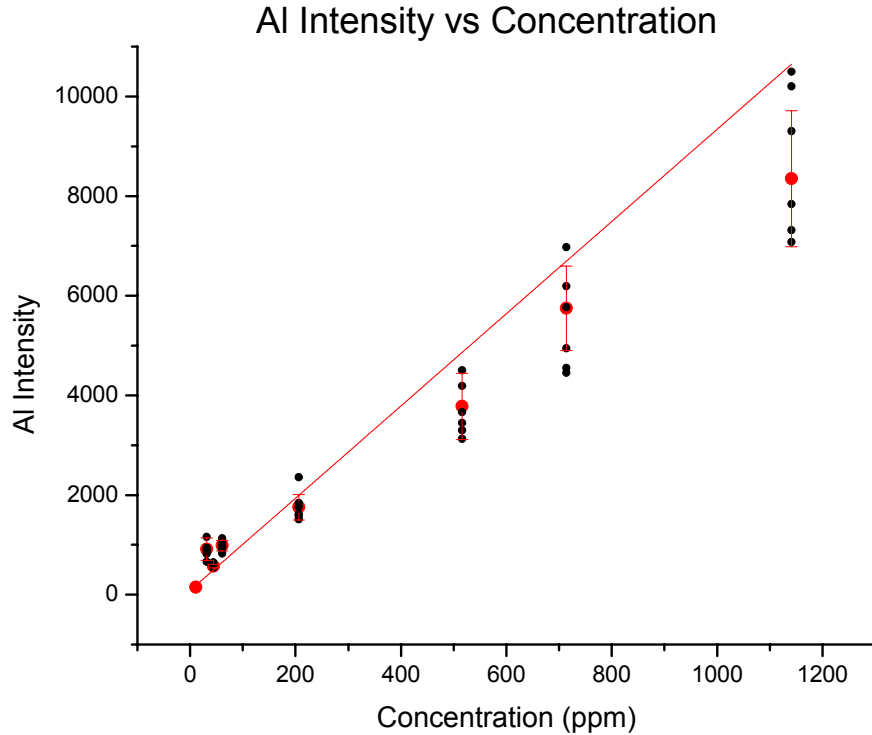


Figure 10. Concentration curve of Al with no reference line (80 mJ/pulse, $\tau_d = 6 \mu\text{s}$).

Limit of Detection

The limit of detection is the lowest concentration at which, ideally, a solute signal can be detected. The common definition in spectroscopy for the limit of a signal is 3σ [18], making the definition for the limit of detection

$$LOD = \frac{3\sigma}{s}, \quad (1)$$

where σ is the average noise of the background, and s is the slope of the calibration curve.

In the case where the signal used in the concentration curve is actually a ratio of two emission lines, this equation must be adjusted:

$$LOD = \frac{3\sigma'}{s'} \quad (2)$$

where

$$\sigma' = \left(\frac{\sigma_1}{x_1} + \frac{\sigma_2}{x_2} + \frac{\sigma_3}{x_3} + \dots \right) / N \quad (3)$$

and

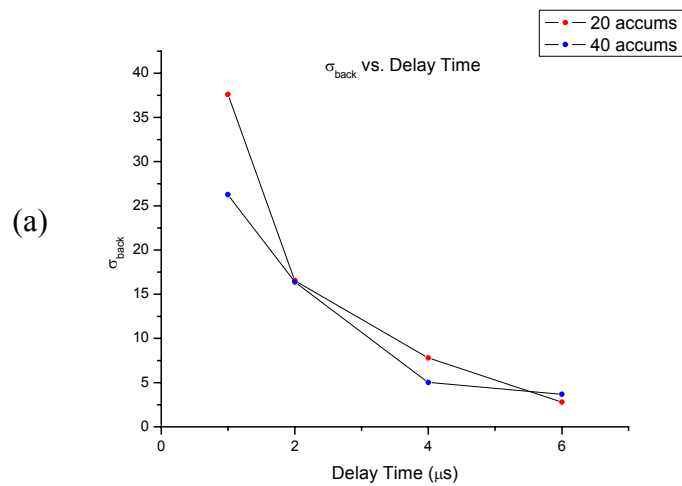
$$s' = \frac{\left(\frac{Al \text{ intensity}}{x} \right)}{\text{concentration}} \quad (4)$$

Here s' is the slope of the Al/Ca concentration curve, x is the reference line, N is the number of points on the concentration curve, and the subscripts stand for the specific σ and x for one concentration. The error on the LOD is calculated by adding the fractional error of the slope and σ in quadrature:

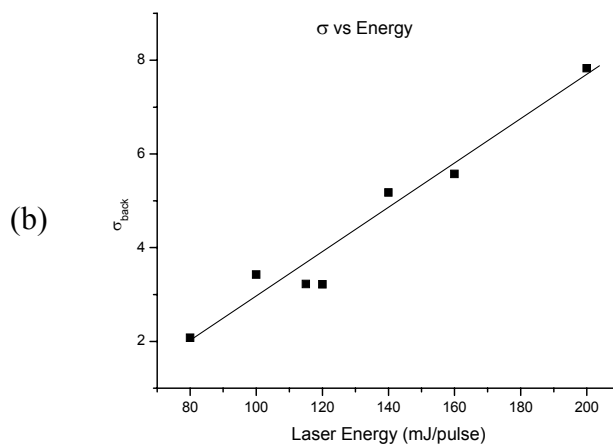
$$\frac{LOD}{\Delta LOD} = \sqrt{\left(\frac{\Delta \sigma}{\sigma} \right)^2 + \left(\frac{\Delta s}{s} \right)^2} \quad (5)$$

Reducing the LOD

Equation 1 shows there are two ways to reduce the limit of detection: increase s or decrease σ . The slope is a result of the natural changes in intensity with concentration and cannot be controlled. The noise, however, can be decreased. Below are two graphs (Figure 11) showing the effects of delay time and laser energy on σ . Increasing delay time and decreasing laser energy caused σ to decrease, and we determined to take measurements 6 μ s after a laser shot of 80 mJ/pulse. Later delay times or lower powers than these decreased the aluminum signal too much for use.



120 mJ



6 μs

Figure 11. The effect of delay time (a) and laser energy (b) on the noise, σ , of the sample.

Final Limits of Detection

Limits of detection were calculated using the concentration shown in Figure 7 and Figure 10. The results are summarized in Figure 12. The limits for both curves are just under 1 ppm, and the non-normalized Al LOD falls within the error bars of the Al/Ca LOD.

	s^*	Δs^*	σ^*	$\Delta \sigma^*$	LOD	ΔLOD
Al/Ca	0.03133	0.00275	0.010321	0.004441	0.988277	0.434026
	s	Δs	σ	$\Delta \sigma$	LOD	ΔLOD
Al	9.25445	0.54148	2.54376	0.096145	0.824606	0.092808

Figure 12. Table of the limit of detection (LOD) and its components for figures __ and __.

Few Accumulation Measurements

The limit of detection is useful because it describes the ability of your method. However, small limits of detection are often created by averaging many measurements covering a large area of the sample. Here, the low LOD required 40 accumulations taken 10 times, and roughly half a square inch of the sample was ablated, which would be harmful to real tissue in an *in vivo* application. Therefore, I studied the ability to detect aluminum using only a single accumulation, meaning 3 OCA at one location. Samples were made at 100 ppm, 10 ppm, 2 ppm, and 0 ppm, and forty individual single accumulation spectra per concentration were recorded and analyzed. The goal was to determine the percentage of spectra that showed aluminum for each concentration. The 0 ppm sample was used to determine how often a noise peak appeared at 396.152 nm when aluminum was not in the material, known as a false positive.

Also a study was done on the effect of taking 2, 3, or 4 accumulations compared to just one. Two to four accumulations would still cause little harm to the tissue. The data was accumulated the extra times by averaging consecutive single accumulation

spectra together before analysis. Again, the data was analyzed to determine what percentage of the time aluminum is seen.

Few Accumulations Data Analysis

Signals for these measurements were much smaller and more sporadic. Figure 13 shows an aluminum signal (which should occur at the second arrow from the left) buried in noise with spikes at other locations resembling emission lines. (The vertical lines below the arrows mark the location of where a peak would be and were added by the program.) For comparison's sake, this is the same range as Figure 6. However, this single accumulation spectrum clearly does not show an aluminum signal above even 1σ .

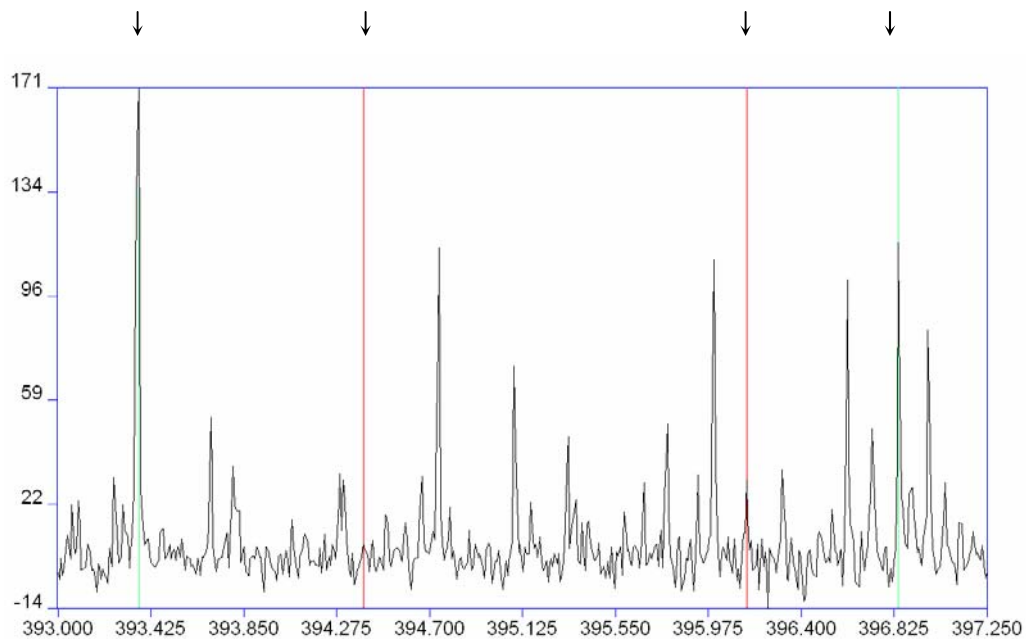


Figure 13. Single accumulation measurement on a 2 ppm Al sample. The two middle arrows denote where the aluminum lines should appear. The outside arrows show the two calcium peaks.

The important criterion was that the ratio of signal to noise be at least greater than one. However, previous intensity calculations returned an area, while the noise is a one

dimensional value. The ratio of the two therefore returns a non-dimensionless value. Instead, the set of three channels around the aluminum signal was averaged. The noise region was also averaged in groups of three. A new standard deviation of the background was calculated from the newly averaged noise region. The average of the three channels around the aluminum 396.152 nm peak was then compared with the new standard deviation. This method worked by assuming that the probability of three consecutive channels being above the noise was slim, unless an aluminum peak occurred, as noise peaks tended to be very narrow. A Matlab program was written to read in the large spectra files and analyze the data as discussed. This program also averaged spectra together to create the multiple accumulation spectra. The code for the program is included in Appendix A.

Data for Few Accumulation Measurements

The following graphs show the percentages of “yes,” aluminum is seen, and “no,” aluminum is not seen. Results were analyzed using three different criteria: signal greater than 1, 3, or 10 σ . A 10 σ criterion catches only the obvious aluminum signals. A 1 σ criterion catches almost all possible aluminum peaks. The decision of which criteria to use depends on the application. For example, in some medical applications, a false negative means a problem is undiagnosed, and a 1 σ test should be used to catch all possibilities of a positive with further testing to detect false negatives. Figure 14 shows the graph for a 3 σ (middle-ground) criterion and shows that this mechanism can detect aluminum in an 100 ppm sample 100% of the time, but only 55% of the time for a 2 ppm concentration. Even when aluminum is not present, as in the 0 ppm sample, a noise peak

occurs at the 396.152 nm position (a false positive) 8% of the time. The error bars represent this 8% uncertainty.

Figure 15 shows the change in percentages with a few more accumulations for a 2 ppm sample. The percentage of “yes” increases by 25% by taking simply 2 accumulations instead of one, with less drastic increases with more accumulations. Clearly it is desirable to take at least one extra accumulation to increase the sensitivity without added much damage to the tissue.

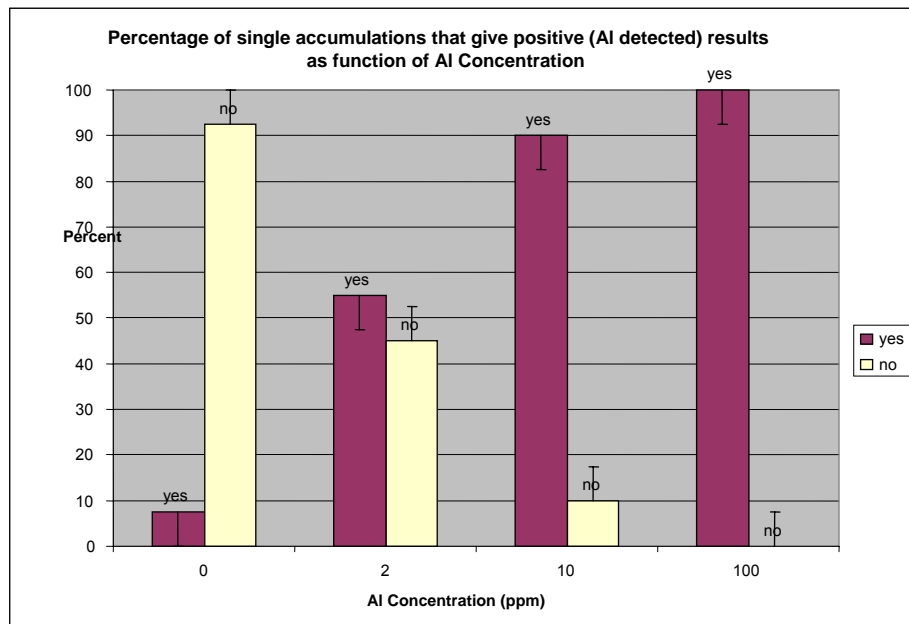


Figure 14. Percentages of “yes” and “no” for a single accumulation system. The criterion for the aluminum signal was 3σ , and the laser energy is 80 mJ/pulse.

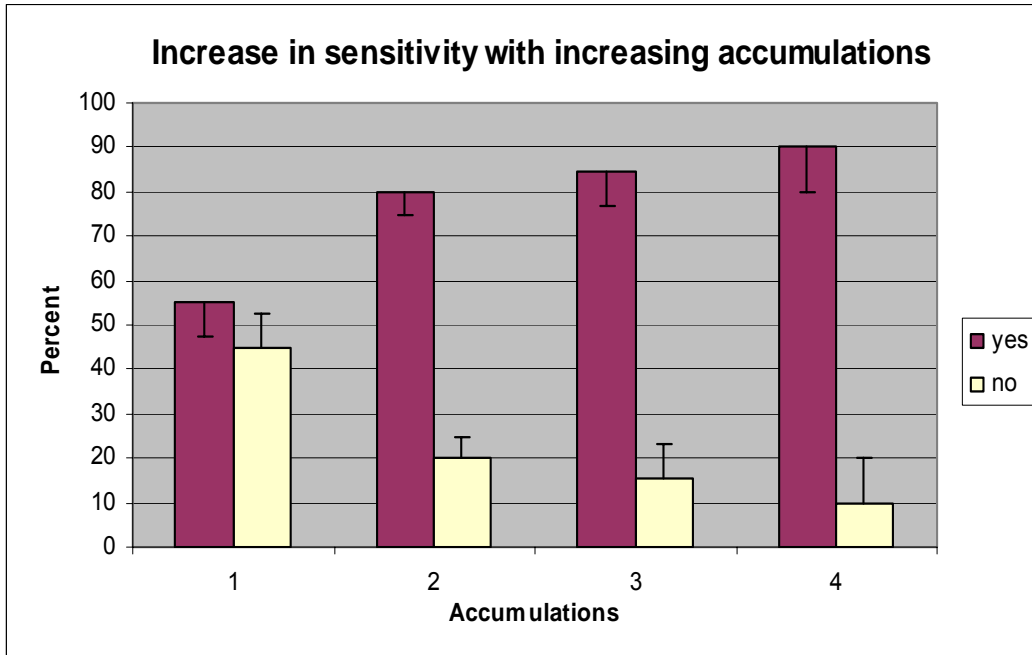


Figure 15. The change in “yes” and “no” percentages with increasing accumulations. The criterion here is Al signal above 3σ , the laser energy is 80 mJ/pulse, and the sample is 2 ppm Al.

Conclusion

This research has shown that Laser-Induced Breakdown Spectroscopy can be used for detecting trace amounts of aluminum in a sample. Aluminum can clearly be seen in a model tissue at the Al 396.1 nm line and the Al 394.4 nm line. Plus, with enough averaging by using many accumulations, aluminum concentration of the sample can be determined. The functional dependence of aluminum line intensity to aluminum concentration is linear for the entire region from 10 ppm to 1000 ppm. A limit of detection was calculated, using the linear concentration curve, to be just better than 1 ppm. If little sample area can be damaged, then aluminum can still be seen 80% of the time by using only two accumulations.

LIBS shows great promise as an elemental analysis tool on human tissue.

Therefore, it is recommended that further research be completed to develop this method for clinical applications. For example, there are difficulties to deal with like the non-uniformities of tissue and unique element concentrations in every person. Also, research is needed to enhance signal strength to lower the limits of detection and to provide the laser light by an optical fiber.

One method for increasing the intensity of a particular line is by using Laser-Induced Fluorescence LIBS, or LIF-LIBS. The method uses a second laser tuned to a narrow band of frequencies around one atomic transition. This laser “pumps” that transition so that the higher state remains populated. With more electrons in the excited state, more can fall into a different transition which you want to increase. For example, referring back to Figure 1, if the $^2S_{1/2}$ to $^2P_{1/2}$ transition is pumped, then many electrons will be excited back into the $^2S_{1/2}$ state. Of those re-excited, 66% of them will fall into the $^2P_{3/2}$, greatly increasing the signal at 396.1 nm. Also, because each atom can be excited and de-excited many times, each atom can now contribute many more photons to be detected. In this way, if any aluminum was available, LIF-LIBS would detect it down to very tiny concentrations. It is not trivial to add this pumping system, for it would require an additional laser to the one currently in use.

Further research should also be done to use optical fiber for laser delivery. This would remove the table-bound optics unrealistic for clinical use. Also, a tiny optical fiber could be inserted into the body without causing much harm. However, there are many difficulties inherent to using optical fiber. For example, it is difficult to couple a powerful pulsed laser into an optical fiber without exceeding the energy threshold of the

fiber. My preliminary research has shown that a multimode, 100 nm core fiber cannot withstand the power utilized in my previous studies. Future developments must include using a high-power, large core fiber and a simple lens for coupling.

This research as shown that there is potential for using LIBS to do elemental analysis in human tissue. By developing ways to enhance the signal and fiber optic delivery, LIBS could become an attractive new tool in clinics for quick and painless procedures. A manuscript of this research was submitted to *Applied Optics* and was accepted in spring 2007 [19].

Bibliography

- [1] S. Koch, W. Garen, M. Müller, and W. Neu, "Detection of chromium in liquids by laser induced breakdown spectroscopy (LIBS)," *Applied Physics A*. **79**, 1071-1073 (2004).
- [2] O. Samek, D.C.S. Beddows, J. Kaiser, S.V. Kukhlevsky, M. Liška, H.H. Telle, J. Young, "Application of laser-induced breakdown spectroscopy to *in situ* analysis of liquid samples," *Optical Engineering* **39 (8)**, 2248-2262 (2000).
- [3] N. Yamaguchi, H. Hotokezaka, S. Nagasaki, and S. Tanaka, "Direct Quantitative Analysis of Particulate Aluminum Suspended in Water Using Laser-Induced Breakdown Spectroscopy," *Soil Sci. Plant Nutr.* **51 (6)**, 911-916 (2005).
- [4] I.V. Cravethi, M. Taschuk, Y.Y. Tsui, and R. Fedosejevs, "Scanning microanalysis of Al alloys by laser-induced breakdown spectroscopy," *Spectrochimica Acta Part B* **59**, 1439-1450 (2004).
- [5] D. Menut, P. Fichet, J-L Lacour, A. Rivoallan, and P. Mauchien, "Micro-laser-induced breakdown spectroscopy technique: a powerful method for performing quantitative surface mapping on conductive and nonconductive samples," *Applied Optics* **42 (30)**, 6063-6071 (2003).
- [6] A. Kumar, F-Y Yueh, J.P. Singh, and S. Burgess, "Characterization of malignant tissue cells by laser-induced breakdown spectroscopy," *Appl. Optics* **43 (28)**, 5399-5403 (2004).

- [7] O. Samek, D.C.S. Beddows, H.H. Telle, J. Kaiser, M. Liška, J.O. Cáceres, A. Gonzáles Ureña, “Quantitative laser-induced breakdown spectroscopy analysis of calcified tissue samples,” *Spectrochimica Acta Part B* **56**, 865-875 (2001).
- [8] M. Baudelet, L. Guyon, J. Yu, J-P Wolf, T. Amodeo, E. Frejafon, P. Laloi, “Spectral signature of native CN bonds for bacterium detection and identification using femtosecond laser-induced breakdown spectroscopy,” *Applied Physics Letters* **88** 063901 (2006).
- [9] Smart Sensors and Integrated Microsystems, Wayne State University, <http://www.ssim.eng.wayne.edu/index.asp>
- [10] Atomic Spectra Database, National Institute of Standards and Technology, <http://physics.nist.gov/PhysRefData/ASD/index.html>
- [11] Kurucz Atomic Line Database, Harvard-Smithsonian Center for Astrophysics, <http://www.cfa.harvard.edu/amdata/ampdata/kurucz23/sekur.html>
- [12] J.A. Aguilera, C. Aragon, “Characterization of a laser-induced plasma by spatially resolved spectroscopy of neutral atom and ion emissions. Comparison of local and spatially integrated measurements,” *Spectrochimica Acta Part B* **59**, 1861-1876 (2004).
- [13] C.M. John and R.W. Odom, “Static secondary ion mass spectrometry (SSIMS) of biological compounds in tissue and tissue-like matrices,” *International Journal of Mass Spectrometry and Ion Processes* **161**, 47-67 (1997).

- [14] B. MacMillan, B. Burke, B. Balcom, and G. Ziegler, "Phantom materials for single point imaging pulse sequences," *Solid State Nuclear Magnetic Resonance* **28**, 106-110 (2005).
- [15] H. Kato, M. Kuroda, K. Yoshimura, A. Yoshida, K. Hanamoto, S. Kawasaki, K. Shibuya, and S. Kanazawa, "Composition of MRI phantom equivalent to human tissues," *Med. Phys.* **32**, 3199-3208 (2005).
- [16] Q. Chen, B. Suki, and K-N. An, "Dynamic Mechanical Properties of Agarose Gels Modeled by a Fractional Derivative Model," *Transactions of the ASME* **126**, 666-671 (2004).
- [17] A. Kumar, F. Y. Yueh, T. Miller, and J. Singh, "Detection of trace elements in liquids by laser-induced breakdown spectroscopy with a Meinhard nebulizer," *Applied Optics* **40**, 6040-6046 (2003).
- [18] J. Ingle Jr., and S. Crouch, *Spectrochemical Analysis* (Prentice Hall, Englewood Cliffs, N.J., 1988), pp. 172-176.
- [19] M.D. Adamson and S.J. Rehse, "Detection of Trace Aluminum in Model Biological Tissue with Laser-Induced Breakdown Spectroscopy," *Applied Optics*, accepted March 2007.

Appendix A. Single Accumulation Analysis Matlab Code

The main Matlab m-file is called *Main.m*. It accepts the data and accumulates spectra together, if desired.

Main.m

```
clear;close all;
fprintf('start \n')

%load the data and put our regions of interest in the regions struct.
regions=loadRegions();

for y = 1:4
    %Average regions together to simulate "accumulation" mode in ESA
    accumNum=y
    %Start by making a matrix
    %Aldata:
    matrix1=zeros(size(regions(1).Aldata,1),size(regions,2));
    for i = 1:size(regions,2)
        matrix1(:,i)=regions(i).Aldata(:,2);
    end
    %Ndata:
    matrix2=zeros(size(regions(1).Ndata,1),size(regions,2));
    for i = 1:size(regions,2)
        matrix2(:,i)=regions(i).Ndata(:,2);
    end
    %Accumulate
    matrix1out=accum(matrix1,accumNum);
    matrix2out=accum(matrix2,accumNum);
    %Reload into a new structure called data
    data = struct('Aldata','Ndata');
    data.Aldata=zeros(size(regions(1).Aldata));
    data.Ndata=zeros(size(regions(1).Ndata));
    for i = 1:size(matrix1out, 2);
        data(i).Aldata(:,2)=matrix1out(:,i);
        data(i).Aldata(:,1)=regions(1).Aldata(:,1);
        data(i).Ndata(:,2)=matrix2out(:,i);
        data(i).Ndata(:,1)=regions(1).Ndata(:,1);
    end

    %Actually chug the data for this accumulation number
    Analyze3(data)
end
```

Main.m first calls *loadRegions*. This file allows the user to select a folder where the full spectrum data is. Then it cuts out the regions of interest, either by asking the user what wavelength region to use or by using default values. The advantage of *loadRegions* is that it cuts the huge spectrum (spe) files from ESAWIN into a manageable size.

loadRegions.m

```
function[regions]=loadRegions()

%load in all the *.spa files from a folder you pick
[filename,pathname]=uigetfile('*.spa','Choose a spa file');
a=dir([pathname,'*.spa']);
values=struct('name','data');
for i=1:size(a,1)
    values(i).name=a(i).name;
    values(i).data=load([pathname,a(i).name]);
end

%Select regions of interest

%Alstart=input(' Enter the starting wavelength for Al region = ');
%Alstop=input(' Enter the last wavelength for Al region = ');
%Noisestart=input(' Enter the starting wavelength for noise region = ');
%Noisestop=input(' Enter the last wavelength for noise region = ');
Alstart=395.5;
Alstop=396.7;
Noisestart=394.8;
Noisestop=395.8;
k=1;
while values(1).data(k)<Alstart
    k=k+1;
end
l=1;
while values(1).data(l)<Alstop
    l=l+1;
end
m=1;
while values(1).data(m)<Noisestart
    m=m+1;
end
n=1;
while values(1).data(n)<Noisestop
    n=n+1;
end
%cut out the regions of interest and put in regions struct
regions=struct('Aldata','Ndata');
for i=1:size(values,2)
    regions(i).Aldata=values(i).data(k:l,:);
    regions(i).Ndata=values(i).data(m:n,:);
end
```

Main.m next calls the *accum* function to do the actual work of accumulating, or averaging, several spectra together.

accum.m

```
function[outMatrix] = accum(matrix, number)

%This function receives a matrix of arrays. It then averages together
%how ever many arrays that you want. For example, accum('matrix of 39
%arrays', 3) returns a structure with 13 arrays each of which is an
average
%of 3 original arrays.

startNum = size(matrix,2);
endNum = floor(startNum/number);
outMatrix = zeros(size(matrix,1),endNum);
for i = 1:endNum
    j = number*(i-1);
    for k = 1:size(matrix,1)
        add = 0;
        for m = 1:number
            add = add + matrix(k,j+m);
        end
        outMatrix(k,i) = add/number;
    end
end
end
```

Main.m then calls the *Analyze3* function which does most of the work. First it takes the data, called *regions*, and “chunks” it by averaging sets of three channels to create a new array for the noise region. It finds the standard deviation and average of the new chunked noise regions. It then checks the noise region to see if the resulting array is following the statistics of a random array. Next, the aluminum signal is found by averaging the three channels around the aluminum peak location, subtracting off the average noise, and dividing by the standard deviation of the noise region. This signal gives how much bigger the aluminum signal is than the noise. The program then looks all the aluminum signals from every spectrum and states how many are above 1σ , 3σ , or 10σ . The aluminum signal is also displayed as a histogram.

Analyze3.m

```
function[]=Analyze3(regions)

%Calculate avg and stdev of noise region as a check (not used)
avgN = zeros(size(regions,2),1);
stdevN = zeros(size(regions,2),1);
for b = 1:size(regions,2)
    [stdevN(b),avgN(b)]=stdev(regions(b).Ndata(:,2));
end

%Average together sets of three channels to create "chunkedN"
```

```

%Then average those averages and find the stdev of them
chunkedN=struct('Ndata','Nstdev');
for i=1:size(regions,2)
    chunkedN(i).Ndata = chunk(regions(i).Ndata);
    [chunkedN(i).Nstdev,chunkedN(i).Navg] = stdev(chunkedN(i).Ndata);
end

%Check the our noise region for credibility
%Subtract background off of chunked data and see what percent is over 1
%sigma, 2 sigma, 3 sigma, and 4 sigma
sig1=zeros(size(chunkedN,2),1);
sig2=zeros(size(chunkedN,2),1);
sig3=zeros(size(chunkedN,2),1);
sig4=zeros(size(chunkedN,2),1);
for i=1:size(chunkedN,2)
    s1=0;s2=0;s3=0;s4=0;
    for j=1:size(chunkedN(i).Ndata,1)
        if abs(chunkedN(i).Ndata(j)-
chunkedN(i).Navg)>(4*chunkedN(i).Nstdev)
            s4=s4+1;
        elseif abs(chunkedN(i).Ndata(j)-
chunkedN(i).Navg)>(3*chunkedN(i).Nstdev)
            s3=s3+1;
        elseif abs(chunkedN(i).Ndata(j)-
chunkedN(i).Navg)>(2*chunkedN(i).Nstdev)
            s2=s2+1;
        elseif abs(chunkedN(i).Ndata(j)-
chunkedN(i).Navg)>(chunkedN(i).Nstdev)
            s1=s1+1;
        end
    end
    var=size(chunkedN(i).Ndata,1);
    sig1(i)=(s1+s2+s3+s4)/var*100;
    sig2(i)=(s2+s3+s4)/var*100;
    sig3(i)=(s3+s4)/var*100;
    sig4(i)=s4/var*100;
end

%Cut out three channel around the Al peak and average them
Center = 396.15;
c=1;
while regions(1).Aldata(c,1)<Center
    c=c+1;
end

Al=zeros(size(regions,2),1);
Alsignal = zeros(size(regions,2),1);
for i = 1:size(regions,2)
    addAl=0;
    for j = (c-1):(c+1)
        addAl = addAl+regions(i).Aldata(j,2);
    end
end

```

```

Al(i)=addAl/3;
Alsignal(i)=(Al(i)-chunkedN(i).Navg)/chunkedN(i).Nstdev;
end
%Determine the number of Al signals above 1sigma, 2*sigma, 3*sigma
yes=zeros(3,1);
no=zeros(3,1);
for i=1:size(Alsignal,1)
    if Alsignal(i)>1
        yes(1)=yes(1)+1;
    end
end
for i=1:size(Alsignal,1)
    if Alsignal(i)>3
        yes(2)=yes(2)+1;
    end
end
for i=1:size(Alsignal,1)
    if Alsignal(i)>10
        yes(3)=yes(3)+1;
    end
end
hist(Alsignal)
yes
for i = 1:3
no(i)=size(Alsignal,1)-yes(i);
end
no
average(sig3)
fprintf('done \n')

```

Analyze.m calls three subroutines called *stdev.m*, *average.m*, and *chunk.m*. As expected, they are used to find the standard deviation of an array, the average of an array, and to “chunk” an array into the averages of three channels.

stdev.m

```

function[Stdev,avg] = stdev(data)

Nsize=size(data,1);
add=0;
for i=1:Nsize
    add = add + data(i);
end
avg = add/Nsize;

add2=0;
for i=1:Nsize
    add2 = add2 + (data(i)-avg)^2;
end
Stdev = sqrt(add2/(Nsize-1));

%This function takes a 1D array of data and calculates the average and

```

```
%stdev of the array.
```

average.m

```
function[avg]=average(array)

add=0;
for i=1:size(array,1)
    add = add + array(i);
end
avg = add/size(array,1);
```

chunk.m

```
function[chunked] = chunk(data)

chunked = zeros(size(data,1)-2,1);
for i=1:(size(data,1)-2)
    add=0;
    for j = i:(i+2)
        add = add + data(j,2);
    end
    chunked(i)=add/3;
end
%This file takes an 2D array and "chunks" it by averaging every three
%channels together from the second column. For example, channels 1,2,3
are
%averaged together to get chunked(1) and then 2,3,4 for chunked(2),
etc.
```
